Closing the Modality Gap for Mixed Modality Search

Anonymous Author(s)

Affiliation Address email

Abstract

Mixed modality search, retrieving information across a heterogeneous corpus composed of images, texts, and multimodal documents, is an important yet un-2 derexplored real-world application. In this work, we investigate how contrastive 3 vision-language models, such as CLIP, perform on the mixed modality search 4 task. Our analysis reveals a critical limitation: these models exhibit a pronounced 5 modality gap in the embedding space, where image and text embeddings form 6 distinct clusters, leading to intra-modal ranking bias and inter-modal fusion failure. To address this issue, we propose GR-CLIP, a lightweight post-hoc calibration 8 method that removes the modality gap in CLIP's embedding space. Evaluated on 9 MixBench, the first benchmark specifically designed for mixed modality search, 10 GR-CLIP improves NDCG@10 by up to 26% over CLIP, surpasses recent vision-11 language generative embedding models by 4%, while using $75 \times$ less compute. 12

1 Introduction

Information in the digital world exists across multiple modalities—text, images, video, audio, and their various combinations. While traditional retrieval systems have primarily focused on searching within a **homogeneous** corpus (e.g., text-to-text or text-to-image retrieval) [27, 15, 17, 26], real-world applications increasingly demand the ability to search and retrieve relevant content across **heterogeneous** modalities (e.g., text-to-{text, image, or both} retrieval) [29]. For instance, a user searching for "Mountain Fuji" might expect to find text documents, standalone images, and multimodal webpages that combine both modalities to describe the mountain (Figure 1a).

Despite its practical importance, the task of **mixed modality search** remains largely underexplored [29]. The central challenge lies in constructing a unified embedding space where semantically similar content across modalities—such as an image and a textual description of "Mountain Fuji"—can be mapped to nearby locations. This enables accurate measurement of semantic similarity between queries and documents, regardless of their modality. Recent advances in multimodal contrastive learning, particularly CLIP-based models [26, 6, 33], offer a promising solution by aligning text and image embeddings through training on large-scale paired image-text datasets.

In this work, we investigate how well these contrastive models perform in realistic mixed modality search scenarios. Specifically, CLIP consists of two separate encoders for vision and language [26]. For each corpus item, we encode image-only and text-only documents using their respective encoders. For multimodal documents containing both image and text, we compute a linear combination of the image and text embeddings to represent them (Figure 1b). Once the embeddings are obtained, we perform similarity search by computing cosine similarity between the query embedding and each corpus item, and evaluate performance using standard retrieval metrics such as NDCG@10 [12], which measures the quality of the top-10 ranked results based on relevance.

Our analysis reveals a fundamental limitation of CLIP-style contrastive models: they exhibit a pronounced **modality gap** [19, 35, 36] in their embedding space, significantly degrading retrieval

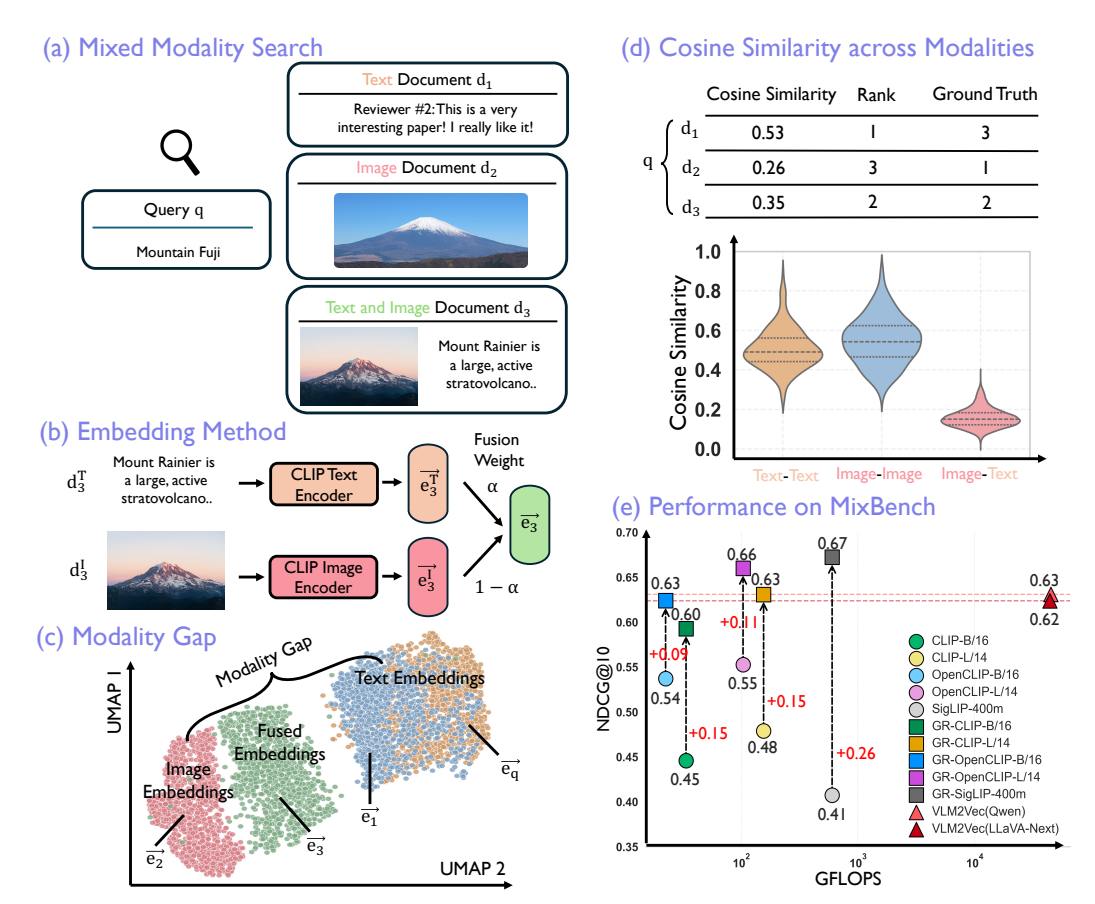


Figure 1: Overview of mixed modality search. (a) Problem Formulation: Mixed modality search aims to retrieve relevant information from a heterogeneous corpus containing multimodal documents. This is achieved by embedding both the query and documents, followed by similarity-based retrieval. (b) Embedding Method: Unimodal documents are embedded using CLIP's modality-specific encoder, while multimodal documents are embedded via a weighted fusion of image and text features. (c) Modality Gap: CLIP's embedding space exhibits a modality gap: embeddings form distinct clusters for each modality and remain largely separated across modalities. (d) Cosine Similarity Across Modalities: Due to this modality gap, documents that share the same modality as the query tend to have higher cosine similarity scores and are ranked higher, introducing systematic ranking bias. (e) Performance on MixBench: On our newly created MixBench benchmark—specifically designed for the task of mixed modality search—GR-CLIP, a lightweight post-hoc calibration method that closes the modality gap, significantly improves performance and outperforms the state-of-the-art VLM2Vec [14] baseline with substantially lower computational cost.

performance in mixed modality settings. Although these models are trained to align image-text pairs, image and text embeddings form separate clusters and remain far apart in the embedding space 39 40 (Figure 1c). This clustering causes a strong *intra-modal ranking bias* (§3), where similarities between items of the same modality (e.g., image-to-image or text-to-text) are much higher than those across 41 modalities (e.g., image-to-text), skewing retrieval rankings (Figure 1d). For instance, given the text 42 query "Mountain Fuji," an image that depicts Mountain Fuji is ranked below an unrelated text snippet 43 like "this is a great paper." Additionally, the modality gap hurts inter-modal fusion (§4): combining 44 image and text embeddings via linear interpolation often pushes the features to a suboptimal region, 45 weakening their semantics and performing worse than using image or text alone. 46

To address the ranking bias and fusion failure caused by the modality gap, we introduce **GR-CLIP**, a lightweight post-hoc calibration method that removes the modality gap in CLIP's embedding space (GR stands for gap-removed). Prior work [35, 36] has shown that the modality gap in CLIP-like models can be approximated by a constant vector that is orthogonal to the image and text embedding subspaces. Based on this theory, we compute the mean embeddings of all image and text data, use

their difference to estimate the modality gap, and subtract this vector from all embeddings before performing retrieval. This method requires only a single pass over the dataset to compute mean embeddings and introduces negligible computational overhead.

Evaluated on **MixBench**, our benchmark explicitly designed for mixed modality search with four subsets (Google-WIT [28], MSCOCO [20], OVEN [11], VisualNews [21]), GR-CLIP consistently outperforms the original CLIP models, achieving up to 26 percentage points improvement in NDCG@10. It also surpasses recent vision-language generative embedding methods such as VLM2Vec [14] by 4 percentage points, while reducing computational cost by 75×. Furthermore, we demonstrate that our method generalizes across different CLIP variants (e.g., OpenAI CLIP [26], OpenCLIP [6], SigLIP [33]) and modalities (e.g., text-to-image, text-to-audio, text-to-video).

In summary, we formulate and study the problem of **mixed modality search**, which reflects realworld scenarios such as web search engines, where users query a heterogeneous corpus containing diverse modality types. We show that state-of-the-art contrastive models suffer from ranking bias and fusion failure due to the modality gap, and we propose a lightweight post-hoc calibration method to address this issue. Our findings highlight the importance of constructing truly unified embedding spaces for effective mixed modality search.

68 2 Preliminaries

71

In this section, we define the mixed modality search task, introduce its challenges and three settings related to the challenge, and describe the methods and evaluation metrics used.

2.1 Problem Formulation

Mixed modality search aims to retrieve semantically relevant content when both the query and the documents may consist of different combinations of modalities, such as text, image, audio, or video. Let $\mathcal M$ be the set of supported modalities (e.g., $\mathcal M=\{\text{text, image, audio, video}\}$). A query is denoted by q, with modality set $m_q\subseteq \mathcal M$. The retrieval corpus is defined as $\mathcal C=\{d_i\}_{i=1}^N$, where each document d_i is associated with a modality set $m_i\subseteq \mathcal M$. The goal is to compute a similarity score $s(q,d_i)$ for each document and return a ranked list based on semantic relevance, regardless of how the modalities are distributed across queries and documents.

Two properties distinguish mixed modality search from traditional retrieval tasks: 1) heterogeneous corpus: the modality composition varies across documents, i.e., there exist $d_i, d_j \in \mathcal{C}$ such that $m_i \neq m_j$. For example, one document may be text-only $(m_i = \{\text{text}\})$, another image-only $(m_j = \{\text{image}\})$, and another multimodal $(m_k = \{\text{text}, \text{image}\})$; b) multimodal documents: some documents contain multiple modalities within a single entry, i.e., $|m_i| > 1$. These modalities often provide complementary information that must be fused for effective understanding (e.g., an image paired with a descriptive caption).

86 2.2 Settings

The combination of a heterogeneous corpus and multimodal documents introduces two central modeling challenges: 1) cross-modal alignment: ensuring that representations of similar concepts are comparable across different modalities—for instance, the text and image of "Mount Fuji" should be embedded in nearby locations in the representation space; 2) multimodal fusion: effectively combining multiple modalities within a document to form a unified, semantically meaningful representation—for example, integrating the text and image of "Mount Fuji" to produce a richer representation of the concept. To study these challenges systematically, we define three settings:

Ablated setting 1: only heterogeneous corpus (§3). Each document is unimodal ($|m_i|=1$), but the corpus spans multiple modalities ($|\mathcal{M}|>1$). For example, it may include text-only and image-only descriptions of the same concept, corresponding to d_1 and d_2 in Figure 1a. This tests only cross-modal alignment—whether the model can encode comparable representations across modalities.

Ablated setting 2: only multimodal documents (§4). All documents contain the same set of modalities ($m_i = \mathcal{M}$ with $|m_i| > 1$). For example, each document includes both an image and a corresponding caption, corresponding to d_3 in Figure 1a. This setting focuses purely on multimodal fusion—evaluating whether the model can effectively combine multiple modalities.

Full setting: mixed modality search (§5). Documents are variably unimodal or multimodal $(|m_i| \ge 1)$, and the corpus is heterogeneous. For instance, some documents may be text-only, others image-only, and others a combination—corresponding to d_1 , d_2 , and d_3 all being present in Figure 1a. This is the most realistic and general setting, reflecting real-world corpora such as news articles, product listings, or scientific datasets. It combines both core challenges and serves as our primary evaluation scenario.

2.3 Methods

Given a query q and a document d_i , we use an embedding model f to compute their embeddings $e_q = f(q)$ and $e_i = f(d_i)$, and rank documents using cosine similarity: $s(q,d_i) = \frac{e_q \cdot e_i}{\|e_q\| \cdot \|e_i\|}$. We evaluate the following embedding approaches:

CLIP (baseline) [26]. CLIP is a contrastive vision-language model trained to align paired image-text inputs. It encodes each modality separately using an image encoder f^I and a text encoder f^T . For unimodal text or image documents d_i and d_j , we use the modality-specific encoder to compute the embedding: $e_i = f^I(d_i)$ and $e_j = f^T(d_j)$. For multimodal documents d_k with image and text inputs d_k^I and d_k^T , we compute a weighted interpolation: $e_k = \alpha \cdot f^T(d_k^T) + (1 - \alpha) \cdot f^I(d_k^I)$, where $\alpha \in [0, 1]$ balances the contribution of each modality.

VLM2Vec (baseline) [14]. VLM2Vec is a state-of-the-art multimodal generative embedding method that adapts large vision-language models f (e.g., LLaVA [23], Qwen-VL [1]) to generate document embeddings in an auto-regressive fashion. Each document d_i is formatted as an instruction-style prompt p_i that combines text and image inputs (e.g., "Generate the embedding for the document: [image tokens] [text tokens]"), which is then processed autoregressively. The pooled representation from the final decoder layer is used as the embedding $e_i = f(p_i)$. This method captures high-level semantic alignment through joint modeling of the two modalities and instruction tuning.

GR-CLIP (ours). Despite CLIP's goal of aligning modalities, prior work reveals a persistent modality gap in its embedding space: image and text embeddings form separate clusters and remain distant [19]. Given a paired image-text embedding e_i^T and e_i^I , their relationship can be modeled as $e_i^T - e_i^I \approx c_\perp$, where c_\perp is a constant vector orthogonal to the shared embedding subspace, representing the modality gap [36]. GR-CLIP (GR stands for gap-removed) is a lightweight post-hoc calibration method that removes this gap by subtracting modality-specific means: $e_i'^T = e_i^T - \mathbb{E}_i[e_i^T], e_i'^I = e_i^I - \mathbb{E}_i[e_i^I]$. This zero-centering eliminates the modality gap [36], as $e_i'^T - e_i'^I = (e_i^T - e_i^I) - (\mathbb{E}_i[e_i^T] - \mathbb{E}_i[e_i^I]) \approx c_\perp - c_\perp = 0$, which improves cross-modal alignment at negligible inference cost. For multimodal documents, we apply the same interpolation over the calibrated embeddings. Figure 1b illustrates this process. In practice, we find this simple calibration significantly boosts CLIP's performance and even outperforms VLM2Vec while using much less compute.

2.4 Evaluation Metrics

We evaluate retrieval performance using **NDCG@10** (Normalized Discounted Cumulative Gain [12]), a widely used metric that reflects both the relevance and ranking of the top-10 retrieved documents. Higher NDCG@10 scores indicate better performance. Details are provided in the Appendix.

140 3 Retrieval with Heterogeneous Corpus

As discussed in §2, we begin with an ablated setting of mixed modality search: a heterogeneous corpus composed of unimodal documents (e.g., text-only or image-only; see Figure 2a). This setting evaluates whether a retrieval model can effectively handle the challenge of cross-modal alignment.

3.1 Dataset Construction

Since no existing dataset follows this setting, we construct new datasets tailored for this task using two complementary strategies: one based on synthetic screenshots and another using image replacements.

Screenshot replacement. Starting from a standard text-only retrieval dataset—where both queries and corpus documents are textual—we synthetically render the text documents as image-based screenshots. Specifically, for each text document d_i^T , we generate a screenshot version d_i^I containing

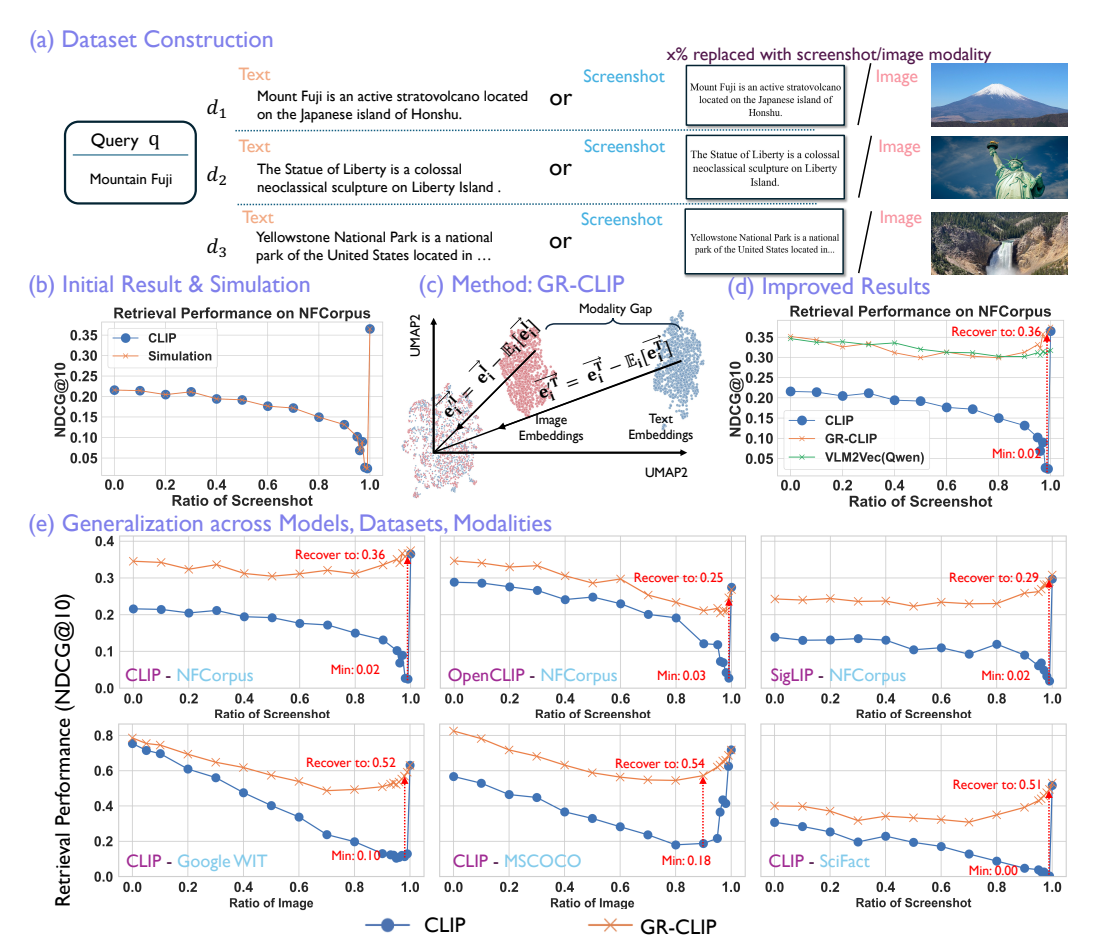


Figure 2: **Retrieval with a heterogeneous corpus.** (a) **Dataset Construction:** We construct a heterogeneous corpus by randomly replacing text documents with either screenshot renderings of the text or paired images with probability p. Since the semantic content remains unchanged, a retrieval system with perfect cross-modal alignment should maintain the same performance regardless of p. (b) **Initial Results & Simulation:** Surprisingly, CLIP exhibits a U-shaped performance curve as text is replaced with screenshots. We attribute this behavior to the modality gap in CLIP's embedding space. A simulation experiment that artificially penalizes cross-modal documents reproduces the same U-shaped trend, confirming our hypothesis. (c) **Method** — **GR-CLIP:** Building on prior work, we propose **GR-CLIP,** a simple post-hoc calibration that removes the modality gap via meancentering of text and image embeddings. (d) **Improved Results:** GR-CLIP flattens the U-shaped curve and significantly improves retrieval accuracy, achieving comparable or better performance than the VLM2Vec baseline with far less compute. (e) **Generalization Across Models, Datasets, and Modalities:** To evaluate generalization, we test GR-CLIP across three CLIP variants, three additional datasets, and three other modalities (detailed in the Appendix). In all cases, the findings and improvements hold consistently.

identical content and replace it with probability p (Figure 2a). This synthetic setup preserves semantic content exactly, making it ideal for controlled experiments. A model with perfect cross-modal alignment should represent paired text and screenshot documents similarly in the embedding space, and thus its retrieval performance should remain unchanged across varying values of p. We apply this transformation to two datasets: NFCorpus [3] and SciFact [30].

Real image replacement. For datasets containing image-caption pairs, we replace text captions d_i^T with their corresponding images d_i^I with probability p. While this setting is more realistic, it introduces slight semantic differences between modalities. Nevertheless, given the underlying semantic alignment, retrieval performance is expected to remain stable across different replacement ratios p. We construct two datasets using this approach: Google WIT [28], MSCOCO [20].

3.2 Initial Results & Simulation

We first focus on the synthetic screenshot-based setting due to its exact semantic preservation. Ideally, a model with perfect cross-modal alignment should yield consistent retrieval performance regardless of how many documents are replaced with screenshots.

Models exhibit a U-shaped performance curve when mixing texts and screenshots. Surprisingly, we observe a U-shaped performance curve (Figure 2b) rather than the expected flat trend. As more screenshots replace text documents (increasing p), performance initially drops—from 0.22 at p=0 (all text) to 0.02 at p=0.99 (99% screenshots). However, at p=1 (all screenshots), performance improves again to 0.36, forming a clear U-shape as a function of p. Interestingly, CLIP performs better on text-to-image retrieval (p=1) than on text-to-text retrieval (p=0), likely due to its training objective: cross-modal contrastive loss, without explicit optimization for unimodal retrieval.

The U-shape arises from the modality gap. We attribute the U-shaped performance to modality gap. First, the modality gap induces intra-modal similarity bias: although CLIP aligns text and image embeddings in a shared space, text and image clusters remain separate (Figure 1c), resulting in systematically higher intra-modal similarity scores (Figure 1d). Second, this bias causes ranking distortion. As screenshots replace more text entries, relevant screenshots are penalized due to lower cross-modal similarity, while irrelevant text documents may rank higher solely because of intra-modal alignment. At p=0.99, the few remaining text documents dominate rankings regardless of relevance. At p=1, all documents are images and modality bias disappears, leading to improved performance—thus forming the U-shaped curve.

Push-down simulation confirms the hypothesis. To verify this explanation, we simulate a modalityinduced ranking bias by assigning a fixed similarity score of zero to all screenshots, effectively
pushing them to the bottom of the ranked list. The resulting performance curve (Figure 2b) closely
matches the actual CLIP curve, validating our hypothesis that the U-shape arises from modality
gap—induced ranking distortion.

3.3 GR-CLIP with Improved Results

185

198

206

Given that the modality gap causes performance drops, we mitigate this gap to improve performance.

Closing the modality gap via mean-shift calibration. Following prior work characterizing the modality gap as a mean shift in the embedding space [36], we propose GR-CLIP, a lightweight post-hoc calibration method. We compute the mean embeddings for text and image modalities and subtract them from their respective representations to center both modalities in the shared space. This reduces separation between modalities (Figure 2d; see §2 for derivation).

Flattened curves and improved performance after removing the modality gap. After applying GR-CLIP, retrieval performance improves significantly, and the U-shaped curve flattens across different p values (Figure 2e). GR-CLIP also outperforms VLM2Vec [14], a recent generative embedding method that achieves similarly flat performance but requires $75 \times$ more computational resources. These results demonstrate that reducing the modality gap is both efficient and effective for improving CLIP-based model in mixed modality retrieval settings.

3.4 Generalization across Models, Datasets, and Modalities

To assess the generality of our findings, we evaluate GR-CLIP across different models, datasets, and modalities. 1) Across models: As shown in Figure 2f (top row), the U-shaped curve is observed across three CLIP variants: OpenAI CLIP [26], OpenCLIP [6], and SigLIP [33]. GR-CLIP consistently flattens the curve and improves performance; 2) Across datasets: As shown in Figure 2f (second row), our findings extend beyond synthetic screenshot settings (NFCorpus [3] and SciFact [30]) to real-world datasets (Google WIT [28] and MSCOCO [20]); 3) Across modalities. We also test generalization to text-to-video and text-to-audio retrieval. Results are provided in the Appendix.

4 Retrieval with Multimodal Documents

We now consider a complementary ablation to §3, where the retrieval corpus is homogeneous, but each document is multimodal—containing both image and text modalities (Figure 3a). This setup

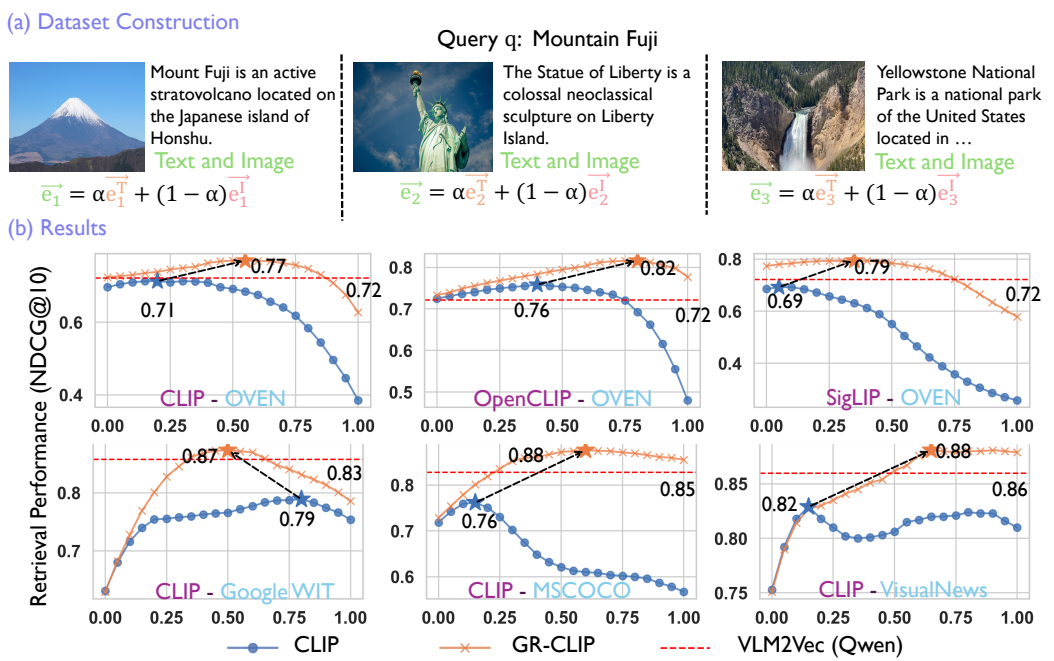


Figure 3: **Retrieval with multimodal documents.** (a) **Dataset Construction:** Each document contains both image and text, and embeddings are obtained by fusing modality-specific features. We vary the fusion coefficient α to evaluate the model's ability to integrate multimodal information. (b) **Results:** GR-CLIP consistently outperforms CLIP across three model variants and four datasets, demonstrating that the modality gap hinders effective multimodal fusion—and that removing it significantly enhances retrieval performance.

evaluates the model's ability to fuse multimodal information, where image and text together should provide richer semantic cues than either modality alone.

4.1 Dataset Construction

We use four real-world multimodal datasets in which each document contains both image and text components. **OVEN** [11] is an existing retrieval benchmark that follow a query-to-multimodal-document format. For **MSCOCO** [20] and **VisualNews** [21], each image is paired with one or more short captions; we randomly sample one caption as the query and generate a long caption using GPT by conditioning on short captions along with the image to form the document. In **Google WIT** [28], each image is accompanied by a title, a short caption, and a long caption. We use the concatenation of the title and short caption as the query, and the image combined with the long caption as the document. These datasets span diverse domains with naturally paired image-text data. Each document provides complementary visual and textual signals, making them well-suited for evaluating modality fusion.

4.2 Results

To analyze how modality fusion is affected by the modality gap, we vary the fusion weight $\alpha \in [0, 1]$, which controls the contribution of each modality for the fused embedding: $e_i = \alpha \cdot e_i^T + (1 - \alpha) \cdot e_i^T$.

Modality gap hinders effective fusion. As shown in Figure 3b (blue curves), with the original CLIP embeddings, performance typically peaks at one of the unimodal endpoints ($\alpha=0$ or $\alpha=1$), and fusion with intermediate α values fails to outperform these unimodal baselines. This suggests that the modality gap prevents effective integration across modalities: linear interpolation often pushes the fused features into a suboptimal region in embedding space, degrading semantic quality and resulting in worse performance than using image or text alone.

Fusion improves significantly after closing the modality gap. Once the modality gap is removed (via mean-shift calibration as described in $\S 3$), fusion becomes substantially more effective. As shown in Figure 3b (orange curves), performance peaks at intermediate α values—surpassing both

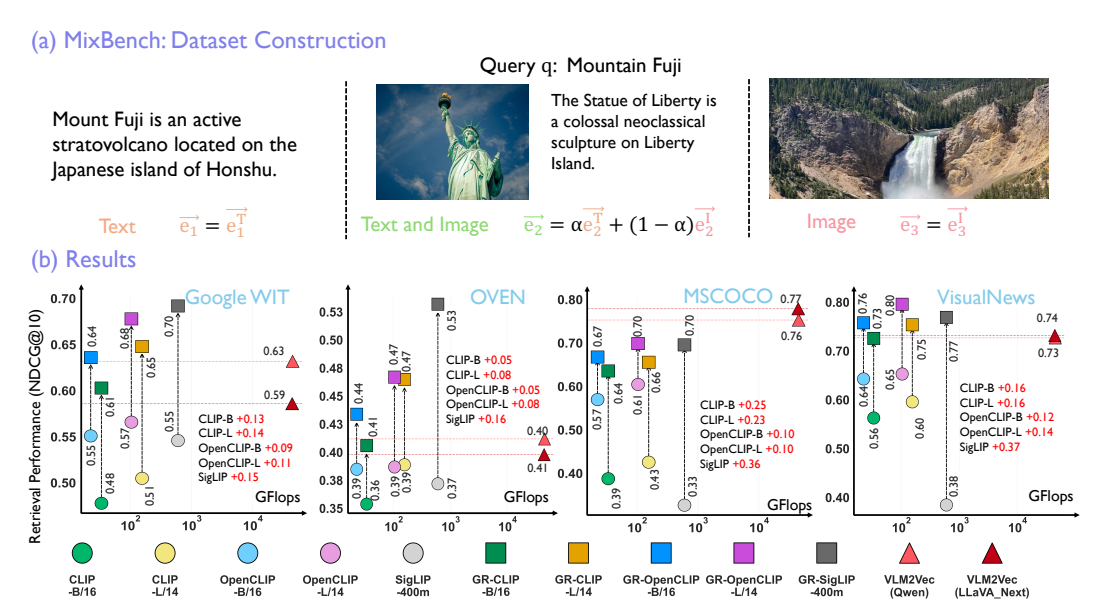


Figure 4: **Mixed modality search.** (a) **Dataset Construction:** We introduce **MixBench**, a benchmark where the corpus is heterogeneous and includes multimodal documents, reflecting the most realistic setting for search engines. (b) **Results:** Across four MixBench subsets and five CLIP variants, GR-CLIP delivers substantial improvements over the original CLIP models by eliminating the modality gap, achieving state-of-the-art performance with significantly lower computational cost.

unimodal baselines. This demonstrates that the gap-removed model, GR-CLIP, successfully integrates complementary information from image and text, yielding stronger overall representations.

Generalization across models and datasets. These findings hold consistently across multiple CLIP variants, including OpenAI CLIP [26], OpenCLIP [6], and SigLIP [33], and across various datasets such as OVEN [11], VisualNews [21], Google WIT [28], and MSCOCO [20]. In all cases, removing the modality gap improves fusion quality, thereby enhancing retrieval performance.

5 Mixed Modality Search

233

244

252

We now unify the findings from §3 and §4 and extend our analysis to the most realistic scenario:
mixed modality search, where documents in the corpus may be purely text, purely image, or a
combination of both (Figure 4a). This setting mirrors real-world search engine challenges, where
retrieval systems must operate over heterogeneous and variably multimodal content.

5.1 MixBench: Dataset Construction

To support research in this realistic setting, we introduce **MixBench**, a new benchmark specifically designed for mixed modality search. MixBench is constructed from four real-world multimodal datasets—**OVEN** [11], **MSCOCO** [20], **Google WIT** [28], and **VisualNews** [21]—which span diverse domains and contain naturally aligned image-text content. The procedure for converting these datasets into a query-document retrieval format is detailed in §4. In MixBench, documents may consist of image-only, text-only, or image-text pairs. To ensure a balanced distribution, we sample document types (pure image, pure text, and multimodal) in a 1:1:1 ratio.

5.2 Results

Figure 4b presents results on the four MixBench subsets using both the original CLIP variants and their gap-removed counterparts (GR-CLIP).

GR-CLIP shows substantial improvement over original CLIP after closing the modality gap.
Consistent with our earlier findings, closing the modality gap via mean-shift calibration leads to signif-

icant performance improvements on MixBench across all tested models, including CLIP [26], Open-CLIP [6], and SigLIP [33]. These improvements generalize across the four datasets—OVEN [11], VisualNews [21], Google WIT [28], and MSCOCO [20]. On average, GR-CLIP achieves up to a 26 percentage point gain in NDCG@10, with negligible additional compute cost. These gains are driven by improved cross-modal alignment and multimodal fusion, as demonstrated in §3 and §4, which are critical for performance in mixed modality retrieval.

GR-CLIP achieves state-of-the-art performance with significantly lower compute. Notably, GR-CLIP outperforms the strong VLM2Vec baseline despite using 75× fewer computational resources.
The only exception is MSCOCO, which VLM2Vec has been trained on, as reported in the paper.
These results underscore the importance of constructing a truly shared embedding space for mixed modality search—a capability that is essential for effective retrieval systems yet often overlooked.

268 6 Related Work

278

279

280

281 282

283

284

285

289

290

291

292

293

294

295

296

297

298

Unimodal, cross-modal and multimodal retrieval. Unimodal retrieval (e.g., text-to-text, image-to-image), cross-modal retrieval (e.g., text-to-image, image-to-text) and multimodal retrieval have been extensively studied in prior work [27, 15, 16, 17, 26, 34, 13] and now power many search engines such as Google and Bing. The core challenge in these settings is to construct an effective representation space that enables accurate similarity comparison between queries and documents. In contrast, we focus on the more complex mixed modality retrieval setting, where both queries and documents may span multiple modalities [29]. This setting is significantly underexplored but highly practical. It presents a new challenge: designing a shared representation space where semantic similarities can be meaningfully measured across modality boundaries.

Multimodal representation learning. Multimodal representation learning aims to unify inputs from different modalities into a coherent embedding space, with early work exploring early fusion and late fusion techniques [25, 18, 5]. Recently, multimodal contrastive learning has emerged as a powerful framework, aligning paired image-text representations through contrastive objectives [10, 26, 33, 6]. Models like CLIP [26], trained on millions of paired examples, have shown remarkable ability to learn semantically aligned embeddings across modalities. More recently, there is growing interest in adapting generative vision-language models (VLMs) for retrieval [14, 8], by repurposing them as embedding models [2, 24]. These models are more flexible and capable of handling diverse multimodal inputs, but often require significantly more computation. In this work, we evaluate both paradigms—CLIP [26] and VLM2Vec [14]—under the mixed modality retrieval setting. Surprisingly, we find that a simple calibration method applied to CLIP can outperform VLM2Vec, despite using far less compute.

Modality gap in multimodal contrastive learning. Recent studies [19, 36, 35] have revealed a persistent modality gap in contrastive multimodal embedding spaces: image and text embeddings tend to cluster separately, even though contrastive learning is designed to align them. This gap has been attributed to a combination of model initialization and contrastive optimization. Theoretically, the modality gap has been characterized as a constant vector orthogonal to both the image and text subspaces [36, 35]. Building on this insight, we adopt a simple but effective mean-reduction calibration, which removes the modality-specific means from embeddings before computing similarity. This lightweight, post-hoc procedure removes the modality gap and leads to substantial gains in the mixed modality search setting.

7 Conclusion

This work addresses the realistic yet underexplored problem of mixed modality search, where queries must retrieve semantically relevant content from a heterogeneous corpus containing multimodal documents. We analyze the behavior of CLIP-based models in this setting and identify a key limitation: a modality gap in the embedding space hinders both cross-modal alignment and multimodal fusion. To address this, we introduce **GR-CLIP**, a simple yet effective method that removes the modality gap and substantially improves retrieval performance. Our findings highlight the importance of truly unified multimodal representations for reliable and efficient mixed modality search.

307 References

- 308 [1] J. Bai, S. Bai, S. Yang, S. Wang, S. Tan, P. Wang, J. Lin, C. Zhou, and J. Zhou. Qwen-vl: A versatile vision-language model for understanding, localization, text reading, and beyond. *arXiv preprint arXiv:2308.12966*, 310 2023.
- [2] P. BehnamGhader, V. Adlakha, M. Mosbach, D. Bahdanau, N. Chapados, and S. Reddy. Llm2vec: Large language models are secretly powerful text encoders. In *COLM*, 2024.
- 313 [3] V. Boteva, D. Gholipour, A. Sokolov, and S. Riezler. A full-text learning to rank dataset for medical information retrieval. In *ECIR*, 2016.
- 315 [4] D. Chen and W. Dolan. Collecting highly parallel data for paraphrase evaluation. In ACL, 2011.
- 136 [5] Y.-C. Chen, L. Li, L. Yu, A. El Kholy, F. Ahmed, Z. Gan, Y. Cheng, and J. Liu. Uniter: Universal image-text representation learning. In *ECCV*, 2020.
- [6] M. Cherti, R. Beaumont, R. Wightman, M. Wortsman, G. Ilharco, C. Gordon, C. Schuhmann, L. Schmidt, and J. Jitsev. Reproducible scaling laws for contrastive language-image learning. In *CVPR*, 2023.
- [7] K. Drossos, S. Lipping, and T. Virtanen. Clotho: An audio captioning dataset. In ICASSP, 2020.
- [8] M. Faysse, H. Sibille, T. Wu, B. Omrani, G. Viaud, C. Hudelot, and P. Colombo. Colpali: Efficient document retrieval with vision language models. In *ICLR*, 2025.
- [9] S. Fu, N. Y. Tamir, S. Sundaram, L. Chai, R. Zhang, T. Dekel, and P. Isola. Dreamsim: Learning new
 dimensions of human visual similarity using synthetic data. In *NeurIPS*, 2023.
- 10] R. Girdhar, A. El-Nouby, Z. Liu, M. Singh, K. V. Alwala, A. Joulin, and I. Misra. Imagebind: One embedding space to bind them all. In *CVPR*, 2023.
- 11] H. Hu, Y. Luan, Y. Chen, U. Khandelwal, M. Joshi, K. Lee, K. Toutanova, and M.-W. Chang. Open-domain visual entity recognition: Towards recognizing millions of wikipedia entities. In *ICCV*, 2023.
- 329 [12] K. Järvelin and J. Kekäläinen. Cumulated gain-based evaluation of ir techniques. TOIS, 2002.
- 133 D. Jiang, R. Zhang, Z. Guo, Y. Wu, jiayi lei, P. Qiu, P. Lu, Z. Chen, G. Song, P. Gao, Y. Liu, C. Li, and H. Li. MMSearch: Unveiling the potential of large models as multi-modal search engines. In *ICLR*, 2025.
- 132 [14] Z. Jiang, R. Meng, X. Yang, S. Yavuz, Y. Zhou, and W. Chen. VLM2vec: Training vision-language models for massive multimodal embedding tasks. In *ICLR*, 2025.
- 1334 [15] V. Karpukhin, B. Oguz, S. Min, P. Lewis, L. Wu, S. Edunov, D. Chen, and W.-t. Yih. Dense passage retrieval for open-domain question answering. In *EMNLP*, 2020.
- 336 [16] O. Khattab and M. Zaharia. Colbert: Efficient and effective passage search via contextualized late interaction over bert. In *SIGIR*, 2020.
- 338 [17] K.-H. Lee, X. Chen, G. Hua, H. Hu, and X. He. Stacked cross attention for image-text matching. In *ECCV*, 339 2018.
- 1340 [18] L. H. Li, M. Yatskar, D. Yin, C.-J. Hsieh, and K.-W. Chang. Visualbert: A simple and performant baseline for vision and language. In *ACL*, 2020.
- [19] V. W. Liang, Y. Zhang, Y. Kwon, S. Yeung, and J. Y. Zou. Mind the gap: Understanding the modality gap
 in multi-modal contrastive representation learning. In *NeurIPS*, 2022.
- [20] T.-Y. Lin, M. Maire, S. Belongie, J. Hays, P. Perona, D. Ramanan, P. Dollár, and C. L. Zitnick. Microsoft
 coco: Common objects in context. In ECCV, 2014.
- [21] F. Liu, Y. Wang, T. Wang, and V. Ordonez. Visual news: Benchmark and challenges in news image
 captioning. In *NeurIPS*, 2021.
- 348 [22] H. Liu, C. Li, Y. Li, B. Li, Y. Zhang, S. Shen, and Y. J. Lee. Llava-next: Improved reasoning, ocr, and world knowledge, January 2024.
- 350 [23] H. Liu, C. Li, Q. Wu, and Y. J. Lee. Visual instruction tuning. In NeurIPS, 2023.
- N. Muennighoff, S. Hongjin, L. Wang, N. Yang, F. Wei, T. Yu, A. Singh, and D. Kiela. Generative representational instruction tuning. In *ICLR 2024 Workshop*, 2024.

- 353 [25] J. Ngiam, A. Khosla, M. Kim, J. Nam, H. Lee, A. Y. Ng, et al. Multimodal deep learning. In *ICML*, 2011.
- [26] A. Radford, J. W. Kim, C. Hallacy, A. Ramesh, G. Goh, S. Agarwal, G. Sastry, A. Askell, P. Mishkin,
 J. Clark, G. Krueger, and I. Sutskever. Learning transferable visual models from natural language
 supervision. In *ICML*, 2021.
- [27] S. Robertson, H. Zaragoza, et al. The probabilistic relevance framework: Bm25 and beyond. Foundations
 and Trends® in Information Retrieval, 2009.
- 359 [28] K. Srinivasan, K. Raman, J. Chen, M. Bendersky, and M. Najork. Wit: Wikipedia-based image text dataset 360 for multimodal multilingual machine learning. In *SIGIR*, 2021.
- Voyage AI. voyage-multimodal-3: all-in-one embedding model for interleaved text, images, and screenshots. Blog post, Nov. 2024.
- 363 [30] D. Wadden, S. Lin, K. Lo, L. L. Wang, M. van Zuylen, A. Cohan, and H. Hajishirzi. Fact or fiction: Verifying scientific claims. In *EMNLP*, 2020.
- [31] Y. Wang, K. Li, Y. Li, Y. He, B. Huang, Z. Zhao, H. Zhang, J. Xu, Y. Liu, Z. Wang, et al. Internvideo: General video foundation models via generative and discriminative learning. arXiv preprint arXiv:2212.03191, 2022.
- 368 [32] Y. Wu, K. Chen, T. Zhang, Y. Hui, T. Berg-Kirkpatrick, and S. Dubnov. Large-scale contrastive language-369 audio pretraining with feature fusion and keyword-to-caption augmentation. In *ICASSP*, 2023.
- 370 [33] X. Zhai, B. Mustafa, A. Kolesnikov, and L. Beyer. Sigmoid loss for language image pre-training. In *ICCV*, 371 2023.
- [34] X. Zhang, Y. Zhang, W. Xie, M. Li, Z. Dai, D. Long, P. Xie, M. Zhang, W. Li, and M. Zhang. Bridging
 Modalities: Improving Universal Multimodal Retrieval by Multimodal Large Language Models. In CVPR,
 2025.
- 375 [35] Y. Zhang, J. Z. HaoChen, S.-C. Huang, K.-C. Wang, J. Zou, and S. Yeung. Diagnosing and rectifying vision models using language. In *ICLR*, 2023.
- 377 [36] Y. Zhang, E. Sui, and S. Yeung-Levy. Connect, collapse, corrupt: Learning cross-modal tasks with uni-modal data. In *ICLR*, 2024.

NeurIPS Paper Checklist

1. Claims

380

381

382

383

384

385

386

387

388

389

390

391

392

393

394

395

396

397

398

399

400

401

402

403

404

405

406

407

408

409

410

411

412

413

415

416

417 418

419

420

421

422

423 424

425

Question: Do the main claims made in the abstract and introduction accurately reflect the paper's contributions and scope?

Answer: [Yes]

Justification: Supporting results are provided in §3, §4, and §5.

2. Limitations

Question: Does the paper discuss the limitations of the work performed by the authors?

Answer: [Yes]

Justification: Limitations are discussed in the Appendix.

3. Theory assumptions and proofs

Question: For each theoretical result, does the paper provide the full set of assumptions and a complete (and correct) proof?

Answer: [NA].

Justification: The paper does not include new theoretical results.

4. Experimental result reproducibility

Question: Does the paper fully disclose all the information needed to reproduce the main experimental results of the paper to the extent that it affects the main claims and/or conclusions of the paper (regardless of whether the code and data are provided or not)?

Answer: [Yes]

Justification: Experimental details are provided in §3, §4, §5, and the Appendix.

5. Open access to data and code

Question: Does the paper provide open access to the data and code, with sufficient instructions to faithfully reproduce the main experimental results, as described in supplemental material?

Answer: [Yes]

Justification: Code is provided via an anonymous GitHub link in the Appendix.

6. Experimental setting/details

Question: Does the paper specify all the training and test details (e.g., data splits, hyper-parameters, how they were chosen, type of optimizer, etc.) necessary to understand the results?

Answer: [Yes]

Justification: Experimental details are provided in §3, §4, §5, and the Appendix.

7. Experiment statistical significance

Question: Does the paper report error bars suitably and correctly defined or other appropriate information about the statistical significance of the experiments?

Answer: [No]

Justification: Reported improvements are large and consistent enough to demonstrate clear significance.

8. Experiments compute resources

Question: For each experiment, does the paper provide sufficient information on the computer resources (type of compute workers, memory, time of execution) needed to reproduce the experiments?

Answer: [Yes]

Justification: Compute resource usage is reported in the Appendix. All experiments are inference-only and require minimal resources.

9. Code of ethics

Question: Does the research conducted in the paper conform, in every respect, with the NeurIPS Code of Ethics https://neurips.cc/public/EthicsGuidelines?

Answer: [Yes]

Justification: We have carefully reviewed and adhered to the NeurIPS Code of Ethics.

10. Broader impacts

Question: Does the paper discuss both potential positive societal impacts and negative societal impacts of the work performed?

Answer: [NA]

Justification: The work does not have direct societal impacts.

11. Safeguards

Question: Does the paper describe safeguards that have been put in place for responsible release of data or models that have a high risk for misuse (e.g., pretrained language models, image generators, or scraped datasets)?

Answer: [NA]

Justification: The paper poses no significant risk of misuse.

12. Licenses for existing assets

Question: Are the creators or original owners of assets (e.g., code, data, models), used in the paper, properly credited and are the license and terms of use explicitly mentioned and properly respected?

Answer: [Yes]

Justification: All external assets are properly cited, and their licenses are respected.

13. New assets

Question: Are new assets introduced in the paper well documented and is the documentation provided alongside the assets?

Answer: [Yes]

Justification: We will release our newly introduced dataset, MixBench, along with documentation.

14. Crowdsourcing and research with human subjects

Question: For crowdsourcing experiments and research with human subjects, does the paper include the full text of instructions given to participants and screenshots, if applicable, as well as details about compensation (if any)?

Answer: [NA]

Justification: The paper does not involve crowdsourcing nor research with human subjects.

15. Institutional review board (IRB) approvals or equivalent for research with human subjects

Question: Does the paper describe potential risks incurred by study participants, whether such risks were disclosed to the subjects, and whether Institutional Review Board (IRB) approvals (or an equivalent approval/review based on the requirements of your country or institution) were obtained?

Answer: [NA]

Justification: The paper does not involve crowdsourcing nor research with human subjects.

16. Declaration of LLM usage

Question: Does the paper describe the usage of LLMs if it is an important, original, or non-standard component of the core methods in this research? Note that if the LLM is used only for writing, editing, or formatting purposes and does not impact the core methodology, scientific rigorousness, or originality of the research, declaration is not required.

Answer: [Yes]

Justification: LLMs were used only for paraphrasing and text refinement, not for the core methodology.

Limitations

- While our work demonstrates that removing the modality gap enables GR-CLIP to achieve substantial 476 performance gains in the mixed modality search setting across diverse datasets, model variants, and modalities, several limitations remain, highlighting valuable directions for future research. First, 478 although we consider a realistic scenario in which documents include both image and text modalities, 479 each document is restricted to a single image and a single text segment. Extending the evaluation to 480 more complex, interleaved multi-image and multi-text documents—such as web pages or scientific 481 articles—could provide a more rigorous and comprehensive assessment. Second, although GR-482 483 CLIP outperforms the generative embedding model VLM2Vec while requiring significantly less 484 computation, it builds on CLIP, which does not model fine-grained modality interaction, and may miss opportunities for deeper cross-modal integration that generative embedding models can capture. 485 Given this, investigating the causes of the modality gap in generative embedding models such as 486 VLM2Vec and developing methods to reduce it presents an important and underexplored research 487 direction toward more powerful and unified multimodal representations. 488
- Nonetheless, our work makes several significant contributions: (1) we are the first to formally define and investigate the mixed modality retrieval setting, where documents of different modalities are retrieved for the same query; (2) we identify the modality gap as a key challenge degrading performance; (3) we propose a simple, theoretically grounded post-hoc calibration that effectively mitigates this gap, consistently boosting performance across CLIP variants and datasets; (4) we introduce MixBench, a benchmark for evaluating retrieval in mixed-modality contexts. Together, these contributions lay a foundation for future advances in this important, emerging area.

496 Code Availability

All code is available at an anonymous GitHub repository, which reproduces all experiments in the paper: https://anonymous.4open.science/r/mixed_modality_search_nips25_workshop_ ReFM.

500 Data Availability

All datasets used in this study are hosted anonymously on Hugging Face to facilitate future research in this emerging area: https://huggingface.co/datasets/mixed-modality-search/ MixBench2025.

504 Compute Resource

All experiments were conducted using a single NVIDIA A100 GPU with 40GB of memory. All experiments are inference-only and require minimal computational resources.

507 Overview

509

511

512

514

- 508 We provide an overview of the Appendix below:
 - §A presents additional generalization results across modalities and evaluation metrics.
 - §B demonstrates the robustness of our method under different settings, including supervised fine-tuning, mean computation, and benchmarks.
 - §C details the methods and includes pseudo-code for reproducibility.
- §D describes the details of the models used.
 - §E explains the evaluation metrics, including NDCG.
 - §F outlines the datasets used and the associated preprocessing steps.
- §G includes case studies comparing CLIP and GR-CLIP on MixBench.

A Generalization across Modalities and Metrics

In the main paper, we show that closing the modality gap significantly improves mixed modality search performance for image-text data, using NDCG@10 as the evaluation metric. Here, we provide additional results to demonstrate: (1) the generalization of our method to modalities beyond image and text, and (2) the robustness of our conclusions under alternative evaluation metrics.

A.1 Generalization across Modalities

Figure 2e in the main paper presents results for the image-text modality. In Figure 5, we extend this analysis to additional modality pairs. Specifically, we report retrieval performance (NDCG@10) for video-text (ViCLIP [31] on the MSVD dataset), audio-text (CLAP [32] on the Clotho [7] dataset), and an additional image-text setting (OpenAI CLIP [26] on the Nights [9] dataset). Across all cases, we observe a consistent U-shaped curve in the original CLIP-based results, which becomes significantly flatter after applying GR-CLIP to remove the modality gap. This trend closely mirrors the behavior observed in the image-text and screenshot experiments in Figure 2e, providing strong evidence of the modality gap's impact and the broad applicability of our method across diverse modalities.

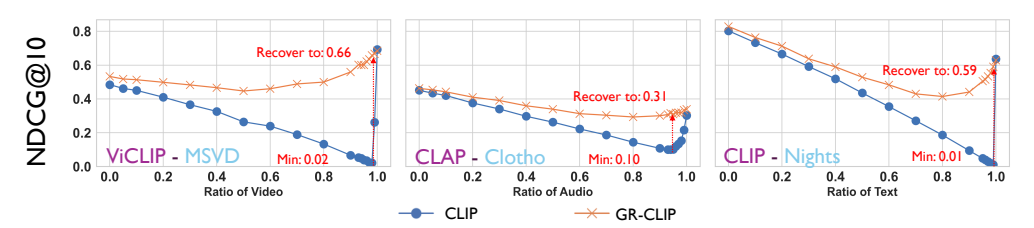


Figure 5: **Generalization across modalities.** GR-CLIP consistently mitigates the U-shaped curve caused by the modality gap and significantly improves performance, demonstrating strong generalizability across diverse modality pairs.

A.2 Generalization across Metrics

In the main paper, we adopt NDCG@10 as the primary evaluation metric. To further assess the robustness of GR-CLIP, we extend our analysis to additional metrics, including NDCG@100 and Recall@1. Table 1 reports results on MixBench across all three metrics, demonstrating that the improvements observed with GR-CLIP are consistent regardless of the evaluation criterion. Figure 6 and Figure 7 further extend the analysis in §3 and §4 using NDCG@100 and Recall@1, respectively, and similarly confirm the consistency of our findings.

Method	Google WIT	MSCOCO	OVEN	VisualNews
CLIP-B/16	0.478/0.505/0.443	0.388/0.426/0.292	0.354/0.398/0.209	0.563/0.604/0.498
CLIP-L/14	0.505/0.516/0.454	0.426/0.490/0.329	0.389/0.431/0.253	0.596/0.656/0.525
OpenCLIP-B/16	0.551/0.563/0.519	0.570/0.615/0.489	0.385/0.426/0.229	0.643/0.693/0.543
OpenCLIP-L/14	0.566/0.585/0.536	0.605/0.662/0.540	0.387/0.445/0.265	0.653/0.733/0.567
SigLIP-400m	0.546/0.566/0.523	0.327/0.374/0.260	0.372/0.428/0.271	0.385/0.475/0.366
VLM2Vec(LLaVANext)	0.586/0.616/0.481	0.769/0.798/0.645	0.398/0.443/0.254	0.744/0.794/0.662
VLM2Vec(Qwen)	0.632/0.660/0.519	0.753/0.778/0.633	0.412/0.467/0.244	0.734/0.784/0.653
GR-CLIP-B/16	0.603/0.642/0.524	0.636/0.690/0.523	0.406/0.459/0.240	0.726/0.768/0.645
GR-CLIP-L/14	0.648/0.678/0.555	0.656/0.708/0.547	0.465/0.523/0.296	0.754/0.770/0.661
GR-OpenCLIP-B/16	0.636/0.666/0.572	0.668/0.751/0.589	0.434/0.490/0.253	0.758/0.783/0.664
GR-OpenCLIP-L/14	0.678/0.704/0.604	0.699/0.784/0.629	0.467/0.525/0.282	0.796/0.814/0.715
GR-SigLIP-400m	0.692/0.722/0.608	0.696/0.732/0.548	0.532/0.581/0.328	0.769/0.793/0.671

Table 1: **Detailed results across all metrics on MixBench.** Each cell reports NDCG@10, NDCG@100, and Recall@1. Best results are highlighted in bold. The consistent performance across metrics demonstrates the robustness of our approach to different evaluation criteria. GR-CLIP underperforms VLM2Vec on MSCOCO because VLM2Vec was trained on MSCOCO.

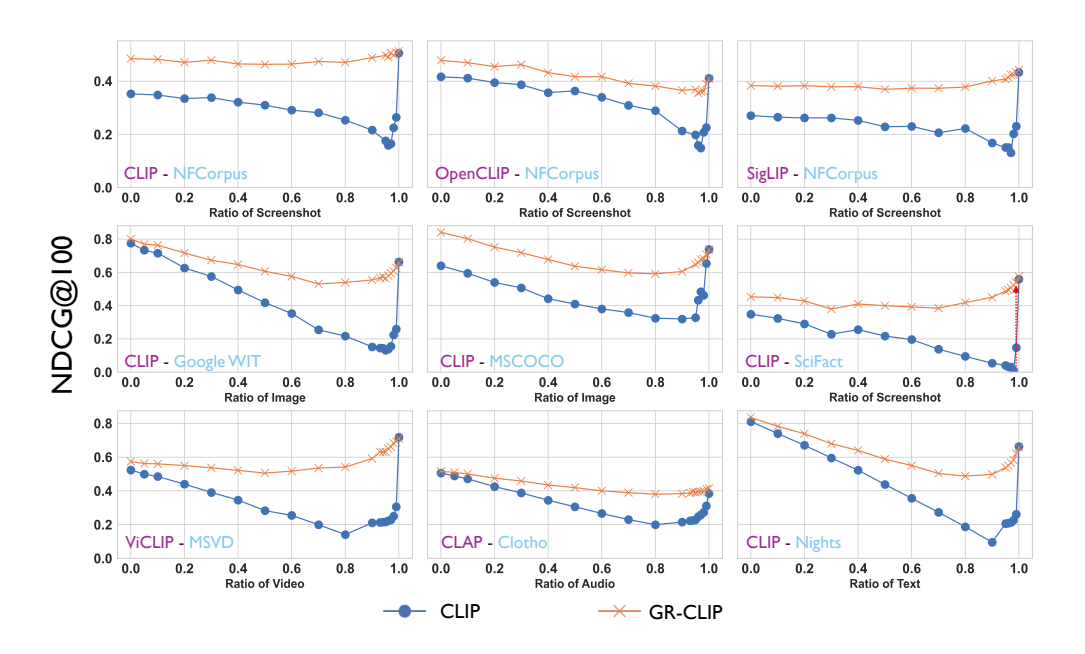


Figure 6: Reproduction of Figure 2 in the main paper using NDCG@100 as the evaluation metric.

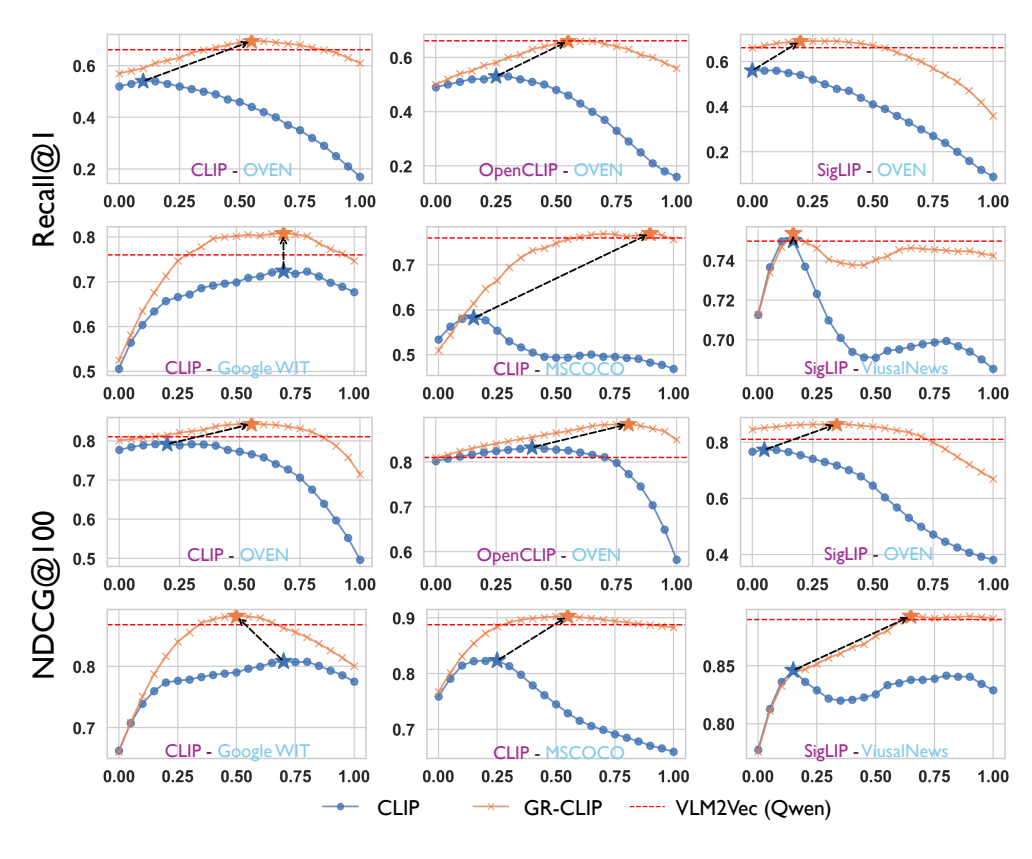


Figure 7: Reproduction of Figure 3 in the main paper using NDCG@100 and Recall@1 as evaluation metrics.

B Method Robustness

539

547

548

549

551

553

555

B.1 Method Robustness to Supervised Fine-Tuning

To assess the applicability of our method after supervised fine-tuning, we fine-tuned the OpenAI CLIP model on the MSCOCO training set (denoted as "-SFT") using a batch size of 64, a learning rate of 5e-5, and the default temperature. We then applied our method to these fine-tuned models. The NDCG@10 scores on MixBench are shown in Table 2.

Model	Google WIT	MSCOCO	OVEN	VisualNews
CLIP-B-SFT	0.489	0.513	0.358	0.588
GR-CLIP-B-SFT	0.617	0.727	0.412	0.745
CLIP-L-SFT	0.514	0.538	0.396	0.612
GR-CLIP-L-SFT	0.656	0.792	0.474	0.772

Table 2: GR-CLIP remains effective with supervised fine-tuned models.

As Table 2 shows, our method consistently improves retrieval performance across all domains, even after supervised fine-tuning, suggesting that the modality gap persists and that our approach remains effective in practical deployment scenarios.

B.2 Method Robustness to Mean-Embedding Computation

To examine our method's robustness to mean-embedding computation, we recomputed the mean embeddings without using any MSCOCO data and then applied GR-CLIP to the MSCOCO dataset. As shown in Table 3, consistent performance improvements were observed across models. Each cell reports NDCG@10 for the base CLIP model, GR-CLIP with MSCOCO access, and GR-CLIP using means computed without MSCOCO. Importantly, the gains persist even when MSCOCO itself is excluded from the mean computation, demonstrating that our approach requires access only to data with the same modality and a similar style, not necessarily the same dataset.

Model	CLIP-B	CLIP-L	OpenCLIP-B	OpenCLIP-L	SigLIP
CLIP	0.388	0.426	0.570	0.605	0.327
GR-CLIP	0.636	0.656	0.668	0.699	0.696
GR-CLIP (w/o access to MSCOCO)	0.624	0.648	0.659	0.687	0.683

Table 3: NDCG@10 on MSCOCO using mean embeddings estimated with and without MSCOCO. GR-CLIP improves over CLIP even without direct access to MSCOCO during mean computation.

We further assessed cross-dataset transfer by computing the query, text, and image embedding means using only 1,000 items from MSCOCO and applying them to VisualNews. As shown in Table 4, we still observed meaningful gains, indicating that our mean-estimation procedure is lightweight, data-efficient, and generalizable across datasets.

Model	CLIP-B	CLIP-L	OpenCLIP-B	OpenCLIP-L	SigLIP
CLIP	0.563	0.596	0.643	0.653	0.385
GR-CLIP	0.726	0.754	0.758	0.796	0.769
GR-CLIP (using 1k items in MSCOCO)	0.678	0.694	0.712	0.742	0.732

Table 4: NDCG@10 on VisualNews using mean embeddings estimated from MSCOCO. GR-CLIP maintains strong performance even when the means are estimated from a small subset (1,000 samples).

B.3 Method Robustness on Benchmarks

 To further demonstrate the robustness of GR-CLIP, we evaluated it on the MMEB benchmark, which contains subsets involving both text—only and image—text retrieval tasks. Unlike our main setting, which focuses on mixed-modality retrieval, MMEB assumes homogeneous corpora in which all candidates share the same modality. Nevertheless, as shown in Table 5, GR-CLIP consistently improves upon CLIP-family baselines across a wide range of subsets. The improvements are particularly strong on datasets containing image—text pairs, such as VisualNews, MSCOCO, and WebQA.

Subset	CLIP-B	CLIP-L	OpenCLIP-B	OpenCLIP-L	SigLIP	VLM2Vec
Subset	CLII-D	CEH-E	оренови-в	Openedii -E	Signii	, E.1.12 vcc
VisualNews_t2i	74.1 / 78.1	76.4 / 79.6	75.4 / 79.3	79.4 / 82.3	52.4 / 57.7	74.4
VisualNews_i2t	73.2 / 77.0	81.3 / 85.3	79.5 / 84.2	82.4 / 86.4	51.3 / 56.4	80.1
MSCOCO_t2i	55.3 / 58.2	58.0 / 63.3	62.4 / 66.5	66.5 / 70.9	58.3 / 64.4	74.5
MSCOCO_i2t	52.8 / 57.4	56.1 / 61.2	60.3 / 64.2	63.2 / 68.4	54.3 / 65.5	72.8
Nights	56.3 / 60.1	67.1 / 69.0	61.7 / 67.1	70.6 / 73.2	63.4 / 68.9	65.5
WebQA	61.0 / 78.3	62.4 / 80.4	64.8 / 82.5	65.2 / 84.3	59.7 / 71.3	86.6
OVEN	42.3 / 66.5	48.5 / 67.9	48.7 / 69.8	50.3 / 71.2	55.3 / 70.7	56.3
FashionIQ	9.7 / 11.5	13.9 / 14.9	12.2 / 16.9	15.4 / 16.7	20.3 / 20.8	16.1
EDIS	75.3 / 90.1	78.9 / 90.7	80.1 / 93.5	82.3 / 92.5	23.7 / 58.7	87.9
WikiSS-NQ	50.6 / 54.2	46.4 / 49.4	54.3 / 57.8	44.0 / 46.2	56.3 / 59.4	58.8
Average (Multimodal Doc Subsets)	59.5 / 78.3	63.3 / 79.7	64.5 / 81.9	65.9 / 82.7	46.2 / 66.9	76.9
Average (All)	55.1 / 63.4	59.5 / 66.4	59.4 / 67.7	61.9 / 69.2	49.5 / 60.0	67.3

Table 5: **Recall@1 results on MMEB datasets.** Each entry is shown as base model / GR-model. GR-CLIP consistently improves CLIP-family models, with the strongest gains on image—text retrieval datasets. Note that VLM2Vec is trained on MSCOCO and WebQA, whereas the CLIP models are not; this in-domain training likely accounts for its superior performance on these benchmarks.

GR-CLIP is evaluated in a zero-shot setting, whereas VLM2Vec is fine-tuned. Subsets such as VisDial and CIRR require dialog understanding or instruction following—tasks that go beyond CLIP's training paradigm. Hence, modality-gap removal alone cannot bridge those task-specific gaps.

C Details of Methods

As introduced in §2.3, GR-CLIP mitigates the modality gap by subtracting global mean vectors for each modality. Specifically, we compute three mean vectors: the query mean \bar{e}_q , the document text mean \bar{e}^T , and the document image mean \bar{e}^I :

$$\bar{e}_q = \mathbb{E}_{q \sim \mathcal{Q}}[f^T(q)], \quad \bar{e}^T = \mathbb{E}_{d^T \sim \mathcal{D}_{\text{text}}}[f^T(d^T)], \quad \bar{e}^I = \mathbb{E}_{d^I \sim \mathcal{D}_{\text{image}}}[f^I(d^I)].$$
 (1)

We distinguish the query mean \bar{e}_q from the text document mean \bar{e}^T to account for structural and semantic differences: queries are often short and interrogative, whereas documents are typically longer and descriptive. This distinction is crucial for reducing alignment bias and improving retrieval performance.

To ensure generalization across datasets and prevent test-set leakage, we compute unified mean vectors from the training sets of multiple datasets, rather than estimating separate means for each dataset using their respective test sets. These unified means are then applied consistently across all test sets.

Query mean (\bar{e}_q) : We sample approximately 10000 text queries from the training splits of MSCOCO, Google WIT, NFCorpus, and VisualNews. These are encoded using f^T and averaged to produce the global query mean \bar{e}_q .

Document text mean (\bar{e}^T) : We sample approximately 10000 long-form text documents or descriptive captions from the training splits of MSCOCO, OVEN, Google WIT, and VisualNews. These are encoded using f^T and averaged to obtain the document text mean \bar{e}^T .

Document image mean (\bar{e}^I): To compute \bar{e}^I , we sample 10000 images from the training splits of MSCOCO, OVEN, Google WIT, and VisualNews. These are encoded using f^I and averaged to produce the document image mean.

OVEN-Specific Query Mean (\bar{e}_q^{OVEN}): Since queries in OVEN are particularly short, we construct a dataset-specific query mean by sampling 2000 queries from the OVEN training split.

Other Modality Means: For non-image-text datasets—such as MSVD (video-text), Clotho (audiotext), and screenshot-style documents (screenshot-text) in SciFact and NFCorpus—we compute modality-specific means using 2500 training examples per modality.

We summarize the full **GR-CLIP** algorithm as follows:

Algorithm 1 GR-CLIP Algorithm

```
Require:
                                                                                                             // Step 3: Encode document embeddings
  1: Calibration sets: Q', D'
                                                                                                     11: for all d_i \in \mathcal{D} do
  2: Query set Q = \{q_1, \dots, q_n\} (text only)
                                                                                                                     if d_i is text then
                                                                                                     12:
                                                                                                                     e_{d_j} \leftarrow f^T(d_j) - \bar{e}^T else if d_j is image then
  3: Document set \mathcal{D} = \{d_1, \dots, d_m\} (text, im-
                                                                                                     13:
        age, or both for each)
                                                                                                      14:
                                                                                                                    else if d_j is image then
e_{d_j} \leftarrow f^I(d_j) - \bar{e}^I
else if d_j = (d_j^T, d_j^I) then
e_{d_j} \leftarrow \alpha f^T(d_j^T) + (1 - \alpha) f^I(d_j^I)
-[\alpha \bar{e}^T + (1 - \alpha) \bar{e}^I]
  4: Pretrained encoders f^T, f^I, interpolation fac-
                                                                                                      15:
        tor \alpha \in [0,1]
                                                                                                      16:
       // Step 1: Pre-compute global means from
                                                                                                      17:
 5: \bar{e}_{q} \leftarrow \mathbb{E}_{q \sim \mathcal{Q}'}[f^{T}(q)]
6: \bar{e}^{T} \leftarrow \mathbb{E}_{d^{T} \sim \mathcal{D}'_{\text{text}}}[f^{T}(d^{T})]
7: \bar{e}^{I} \leftarrow \mathbb{E}_{d^{I} \sim \mathcal{D}'_{\text{image}}}[f^{I}(d^{I})]
                                                                                                      18:
                                                                                                                     end if
                                                                                                      19:
                                                                                                     20: end for
                                                                                                     // Step 4: Retrieval 21: s(q_i, d_j) \leftarrow \frac{e_{q_i} \cdot e_{d_j}}{\|e_{q_i}\| \cdot \|e_{d_j}\|}
       // Step 2: Encode query embeddings
8: for all q_i \in \mathcal{Q} do
9: e_{q_i} \leftarrow f^T(q_i) - \bar{e}_q
10: end for
                                                                                                     22: Ranks \leftarrow argsort(s, descending)
                                                                                                     23: return Ranks
```

D Details of Models

- In this section, we provide the exact versions and checkpoint links for all models used in our
- experiments. For CLIP-based models, we include two variants of **OpenAI CLIP** [26], two variants
- of **OpenCLIP** [6], and **SigLIP-400M** [33].
- For the VLM2Vec framework, we use two variants: one based on LLaVA-Next [22], which serves
- as the backbone for the results reported in the main paper [14]; and another based on the latest
- officially released **Qwen-VL** [1], which achieves the best performance on the MMEB [14] benchmark
- according to its official repository.

608

610

611

- Additionally, for non-image-text modalities, we use ViCLIP[31] for video-text retrieval and
- 606 **CLAP**[32] for audio-text retrieval tasks.
- 607 All model checkpoint links are listed below:
 - OpenAI CLIP-B/16: https://huggingface.co/openai/clip-vit-base-patch16
- OpenAI CLIP-L/14: https://huggingface.co/openai/clip-vit-large-patch14-336
 - OpenCLIP-B/16: https://huggingface.co/laion/CLIP-ViT-B-16-laion2B-s34B-b88K
 - OpenCLIP-L/14: https://huggingface.co/laion/CLIP-ViT-L-14-laion2B-s32B-b82K
- **SigLIP-400m**: https://huggingface.co/google/siglip-so400m-patch14-384
 - VLM2Vec (LLaVA-Next): https://huggingface.co/TIGER-Lab/VLM2Vec-LLaVa-Next
- VLM2Vec (Owen-VL): https://huggingface.co/TIGER-Lab/VLM2Vec-Owen2VL-7B
- ViCLIP-L/14: https://huggingface.co/OpenGVLab/ViCLIP-L-14-hf
- CLAP: https://huggingface.co/laion/clap-htsat-fused

817 E Details of Evaluation Metrics

- In the main paper, we use the widely adopted NDCG@10 as the evaluation metric. Here, we provide
- the detailed computation process for this metric.
- Given a ranked list of retrieved items up to position K, NDCG@K is computed as:

$$NDCG@K = \frac{1}{IDCG@K} \sum_{i=1}^{K} \frac{2^{rel_i} - 1}{\log_2(i+1)}$$
 (2)

- where rel_i denotes the relevance score of the item at rank i, and IDCG@K is the ideal DCG—that is,
- the maximum possible DCG for the top K items—computed by sorting the items by relevance in
- 623 descending order:

IDCG@
$$K = \sum_{i=1}^{K} \frac{2^{\text{rel}_{i}^{\star}} - 1}{\log_{2}(i+1)}$$
 (3)

- where rel $_i^{\star}$ is the *i*-th highest relevance score in the ideal ranking.
- NDCG@10 ranges from 0 to 1, with 1 indicating a perfect ranking.

F Details of Datasets

- 627 In this section, we provide additional details on how each dataset is processed to support our retrieval
- experiments in §3, 4, and 5. For each dataset, we distinguish between the original data format (Before)
- and the modified version used in our framework (After). We also describe the key post-processing
- 630 steps.

NFCorpus [3], SciFact [30]:

- 632 Before: A short text query paired with a relevant long text document.
- 633 After: We retain the short text query and render the long text document into a screenshot using
- 634 OpenCV. This allows retrieval of either the original text document or its rendered screenshot given
- 635 the query.

636 **Google WIT [28]:**

- ⁶³⁷ Before: Each sample includes a page title, a long page description, a reference image, and a reference
- 638 description for the image.
- 639 After: We concatenate the page title and image reference description to form the query. The page
- description is used as the long text document, and the associated image serves as the image document.

641 **OVEN [11]:**

- 642 Before: Each query consists of an image-text pair, and the retrieval target is also an image-description
- 643 pair.
- 644 After: Since either the image or text component can independently answer the query, we treat both
- the image and caption as valid standalone documents. The query remains unchanged.

646 MSCOCO [20]:

- 647 Before: Each image is paired with five captions.
- 648 After: One caption is sampled as the query. The remaining captions are used to construct a long-form
- description via GPT-40, with the content of the sampled caption preserved. This long description
- becomes the text document, and the associated image serves as the image document.

651 VisualNews [21]:

- 652 Before: Each image is paired with a short news-style caption.
- 653 After: We use GPT-40 to jointly analyze the image and its associated article from the original
- VisualNews dataset. Based on both the visual content and article text, GPT-40 generates a detailed
- descriptive paragraph that expands upon the original caption, which we use as the text document. The
- image serves as the image document, and the original caption is retained as the query.

657 **Clotho** [7]:

- 658 Before: Each audio clip is paired with several semantically similar captions.
- 659 After: One caption is selected as the query, and another semantically similar caption (chosen by
- 660 GPT-40) is used as the text document. The audio clip itself is used as the audio document.

661 MSVD [4]:

- 662 Before: Each video is paired with several semantically similar captions.
- 663 After: One caption is used as the query, and another semantically similar caption (chosen by GPT-40)
- serves as the text document. The video is treated as the video document.

665 Nights [9]:

- 666 Before: Each image is paired with a visually similar image.
- 667 After: One image is used as the query. GPT-40 observes this image and generates a concise title,
- which we use as the text document. The paired image serves as the image document.
- 669 VLM2Vec input format: For VLM2Vec [14], prompts are required to serve as instructions for gener-
- ating embeddings. Specifically, for each *Query*, we use the prompt "Retrieve a relevant item
- 671 that represents: {Query}\n'' in settings 1 and 3, which involve retrieval from a heterogeneous
- corpus composed of multiple modalities. In Setting 2, where retrieval is over a homogeneous corpus of
- 673 fused image-text pairs, we use "Retrieve an image-description pair that represents:
- 674 {Query}\n''. Documents follow the format specified in the original datasets.
- 675 **CLIP input format:** For **CLIP**-based models [26, 33, 6, 31, 32] and **GR-CLIP**, we do not apply
- any instructions. Queries and documents are directly passed to the respective CLIP text and image
- encoders without modification.

Table 6 summarizes the key characteristics of each dataset, including the retrieval setting, the modality composition of queries and corpora, and the total number of evaluation examples.

Dataset	Queries	Documents	Setting No.	# of Queries	# of Documents
Google WIT [28]	T	T / I / I + T	1,2,3	1000	4423
OVEN [11]	T + I	T/I/I+T	1,2,3	1000	1000
MSCOCO [20]	T	T/I/I+T	1,2,3	984	984
VisualNews [21]	T	T/I/I+T	1,2,3	981	981
SciFact [30]	T	T/S	1	300	5183
NFCorpus [3]	T	T/S	1	323	3633
MSVD [4]	T	T/V	1	670	670
Clotho [7]	T	T / A	1	1046	1046
Nights [9]	I	I/T	1	1000	1000

Table 6: **Overview of datasets used in our experiments.** For each dataset, we indicate the retrieval setting, the modalities involved in queries and documents (T = text, I = image, S = screenshot, V = video, A = audio), and the number of query-document pairs used for evaluation.

G Case Studies

Below, we present case studies from each subset of MixBench, which also serve as visualizations of our dataset. For each example query, we display the Top-5 retrieved results from both the baseline OpenAI CLIP-L/14 and our proposed GR-CLIP-L/14 model. Each retrieved document is annotated with its modality (text, image, or multimodal), its cosine similarity to the query, and whether it is a ground-truth relevant item.

These example results illustrate both the diversity of the MixBench datasets and the effectiveness of GR-CLIP in mixed modality search. Unlike the original CLIP model, which tends to retrieve documents matching the query's modality, GR-CLIP successfully bridges the modality gap, retrieving results that more accurately reflect the semantic intent of the query—regardless of modality.

G.1 Google WIT

Query: List of Jews in sports, Nate Ebner 691

692 **CLIP Top-5 Results** 693

702

708

- Rank No.1, Cosine Similarity = 0.5430, Modality = text 694
- This is a list of individuals currently serving in the United States House of Representatives. 695
- 696 Rank No.2, Cosine Similarity = 0.5355, Modality = text697
- 698 This is a list of notable Austrians.
- 699 ______
- Rank No.3, Cosine Similarity = 0.5227, Modality = text 700
- This is a list of vehicles manufactured by the Buick Motor Division of General Motors. 701
- _____ Rank No.4, Cosine Similarity = 0.5181, Modality = text703
- This is a list of notable alumni and faculty of Golden Gate University. 704
- 705
- Rank No.5, Cosine Similarity = 0.5101, Modality = text 706
- Puthenchira is a village in Thrissur district in the state of Kerala, India. 707

GR-CLIP Top-5 Results 709

Rank No.1, Cosine Similarity = 0.3403, Modality = Image (Ground Truth)



711

Rank No.2, Cosine Similarity = 0.1798, Modality = text712

This is a list of notable Austrians.

Rank No.3, Cosine Similarity = 0.1774, Modality = text 715

The Lebanon national football team, controlled by the Lebanese Football Association, have repre-716 sented Lebanon in association football since their inception in 1933. The squad is governed by the 717 Asian Football Confederation continentally, and FIFA worldwide. While Lebanon have yet to qualify 718 for the FIFA World Cup, they have participated twice in the Asian Cup: in 2000, when they hosted the 719 event, and in 2019, the first time through regular qualification. Lebanon's main venue is the Camille 720 Chamoun Sports City Stadium in Beirut; however they also play in other locations such as the Saida 721 International Stadium in Sidon. In 1934, Lebanon played their first match against the Romanian side 722 CA Timisoara, but it was not ratified by FIFA. Lebanon played their first FIFA-recognised game 723 in 1940 against Mandatory Palestine. During their 2014 qualification campaign for the World Cup, 724 Lebanon reached the final qualifying round for the first time thanks to a 2–1 victory against South 725 Korea at home in 2011, but failed to qualify for the 2014 FIFA World Cup finishing bottom of their 726 group. At the 2019 Asian Cup, Lebanon were close to qualifying to the knock-out stages for the first 727

728 time. 729 730

Rank No.4, Cosine Similarity = 0.1723, Modality = text

This is a list of properties and historic districts in Winchester, Massachusetts, that are listed on the National Register of Historic Places. The locations of National Register properties and districts may be seen in an online map by clicking on "Map of all coordinates." This National Park Service list is complete through NPS recent listings posted July 17, 2020.

______ 735

Rank No.5, Cosine Similarity = 0.1708, Modality = multimodal 736



731

732

733

734

737

This list is of that portion of the National Register of Historic Places designated in Essex County, Massachusetts. The locations of these properties and districts for which the latitude and longitude coordinates are included below, may be seen in a map. There are more than 450 designated properties in the county, including 25 that are further designated as National Historic Landmarks. The municipalities of Andover, Gloucester, Ipswich, Lawrence, Lynn, Methuen, and Salem are to be found on a separate list of the more than 200 identified here, except two properties are split between Methuen and Lawrence, and one between Lynn and Nahant; these entries appear on more than one list. This National Park Service list is complete through NPS recent listings posted August 14, 2020.

G.2 MSCOCO

Query: A woman in a room with a cat.

CLIP Top-5 Results

739

740

741

756

757

763

764

769

742 Rank No. 1, Cosine Similarity = 0.5044, Modality = text

A kitchen featuring light wood cabinets and a black granite countertop. It includes a black stove with four burners, an over-the-range microwave, and a black refrigerator. The flooring is a warm wooden tone.

745 tone.

746

747 Rank No.2, Cosine Similarity = 0.4605, Modality = text

A cat is perched on the closed lid of a toilet, appearing somewhat perturbed. The toilet is located in a bathroom with a light-colored wall. Next to the toilet, there is a basket or container. The cat's tail is visible, and it seems to be alert or possibly startled.

751

752 Rank No.3, Cosine Similarity = 0.4445, Modality = text

A long hot dog is placed in a bun on a white paper plate, which sits on a wooden table. The hot dog extends beyond the ends of the bun.

755

Rank No.4, Cosine Similarity = 0.4160, Modality = multimodal



The warm and cozy living room is adorned with Christmas decorations, featuring a silver tinsel Christmas tree by the fireplace. The room is filled with a variety of gift-wrapped presents scattered around on the red carpet. On the mantelpiece, festive ornaments and stockings add to the holiday spirit. A comfortable beige sofa with cushions sits alongside a coffee table with magazines. The ceiling is decorated with shimmering golden stars, and a television displaying a dartboard game adds to the lived-in, festive atmosphere. The soft lighting from lamps enhances the room's inviting ambiance.

758

759 Rank No.5, Cosine Similarity = 0.4126, Modality = text

A delicious Italian pizza is presented on a white plate, topped with slices of fresh tomatoes, green olives, and thinly sliced onions. The pizza is garnished with herbs and seasonings, adding a colorful and flavorful touch to the dish.

GR-CLIP Top-5 Results

765 Rank No. 1, Cosine Similarity = 0.3012, Modality = multimodal (**Ground Truth**)



A woman is standing in a kitchen, smiling and holding a cat. She is wearing a brown sweater and a blue plaid skirt. The kitchen has wooden cabinets and a countertop with a potted plant and a bowl of oranges. There is a sink with dishes on one side and a white refrigerator on the other. A clock is visible on the wall, and there are various items on the counter and a small rug on the floor.

Dark N. 2. Caring Similarity, 0.2024, Madelity, analysis and

Rank No.2, Cosine Similarity = 0.2924, Modality = multimodal



A person wearing glasses and a black shirt is sitting by a window with closed blinds, brushing a cat that is sitting on a purple blanket draped over a radiator. The cat is facing away, and the brush is Magenta with a grey bristle area. The floor is wooden, and the cat seems relaxed.

771 Rank No.3, Cosine Similarity = 0.2780, Modality = text

A cat is perched on the closed lid of a toilet, appearing somewhat perturbed. The toilet is located in a bathroom with a light-colored wall. Next to the toilet, there is a basket or container. The cat's tail is

visible, and it seems to be alert or possibly startled.

775

776 Rank No.4, Cosine Similarity = 0.2745, Modality = multimodal



A gray armchair and a black armchair are positioned next to each other in a room. A small lamp is placed on a table next to the black chair. Partially visible from behind the armchair is a cat peeking out, adding a playful touch to the setting. In front of the chairs, there is a wooden table with a remote control on it.

778

Rank No.5, Cosine Similarity = 0.2612, Modality = image



G.3 OVEN

82 *Query:*



What is the name of this building?

783 784

CLIP Top-5 Results

Rank No.1, Cosine Similarity = 0.5340, Modality = multimodal

786

785



Clérigos Church. The Clérigos Church is a Baroque church in the city of Porto, in Portugal. Its 75-meter-tall bell tower, the Torre dos Clérigos, can be seen from various points of the city and is one of its most characteristic symbols. History: The church was built for the Brotherhood of the Clérigos (Clergy) by Nicolau Nasoni, an Italian architect and painter who left an extensive body of work in the north of Portugal during the 18th century. Construction of the church began in 1732 and was finished in 1750, while the bell tower and the monumental divided stairway...

787

Rank No.2, Cosine Similarity = 0.5321, Modality = image



789

Rank No.3, Cosine Similarity = 0.5276, *Modality* = multimodal

791 792



St. Peter's Basilica. The Papal Basilica of Saint Peter in the Vatican, or simply Saint Peter's Basilica, is a church built in the Renaissance style located in Vatican City. It was initially planned by Pope Nicholas V and then Pope Julius II to replace the aging Old St. Peter's Basilica, which was built in the fourth century by Roman emperor Constantine the Great. Construction of the present basilica began on 18 April 1506 and was completed on 18 November 1626. Designed principally by Donato Bramante, Michelangelo, Carlo Maderno, and Gian Lorenzo Bernini...

793

Rank No.4, Cosine Similarity = 0.5274, Modality = multimodal

795



Coit Tower. Coit Tower is a 210-ft tower in the Telegraph Hill neighborhood of San Francisco, California, offering panoramic views over the city and the bay. Built between 1932 and 1933 using Lillie Hitchcock Coit's bequest to beautify the city, it was added to the National Register of Historic Places in 2008. The unpainted reinforced concrete tower, designed by Arthur Brown, Jr. and Henry Howard, features American fresco mural paintings by 25 different onsite artists...

796 797

Rank No.5, Cosine Similarity = 0.5252, Modality = multimodal

798



Ilinden (Memorial). Also known as Makedonium, Ilinden is a monument in Kruševo, North Macedonia. Officially opened on August 2, 1974, it commemorates the Second Session of the Anti-fascist Assembly and the 1903 Ilinden uprising. Designed by Jordan and Iskra Grabuloski, it honors fighters in the National Liberation Struggle from 1941–1944. Description. The monument covers 12 acres and features a rounded architectural style...

GR-CLIP Top-5 Results

801 Rank No.1, Cosine Similarity = 0.3153, Modality = text (**Ground Truth**)

Canadian National Vimy Memorial. The Canadian National Vimy Memorial is a war memorial site in France dedicated to the memory of Canadian Expeditionary Force members killed during the First World War. It also serves as the place of commemoration for Canadian soldiers of the First World War killed or presumed dead in France who have no known grave. The monument is the centrepiece of a 100 (ha) preserved battlefield park that encompasses a portion of the ground over which the Canadian Corps made their assault during the initial Battle of Vimy Ridge offensive of the Battle of Arras.

810 Rank No.2, Cosine Similarity = 0.2795, Modality = image



811

814

809

813 Rank No.3, Cosine Similarity = 0.2762, Modality = multimodal



Mary, Queen of the World Cathedral. Mary, Queen of the World Cathedral or in full Mary, Queen of the World and St. James the Great Cathedral is a minor basilica in Montreal, Quebec, Canada, and the seat of the Roman Catholic archdiocese of Montreal. It is the third largest church in Quebec after Saint Joseph's Oratory (also in Montreal) and the Basilica of Sainte-Anne-de-Beaupré east of Quebec City. The building is 101 m (333 ft) in length, 46 m (150 ft) in width, and a maximum height of 77 m (252 ft) at the cupola, the diameter of which is 23 m (75 ft).

Rank No.4, Cosine Similarity = 0.2744, Modality = image



817

819 820

815

 $Rank\ No.5,\ Cosine\ Similarity = 0.2590,\ Modality = multimodal$



Sydney Town Hall. The Sydney Town Hall is a late 19th-century heritage-listed town hall building in the city of Sydney, the capital city of New South Wales, Australia, housing the chambers of the Lord Mayor of Sydney, council offices, and venues for meetings and functions. It is located at 483 George Street, in the Sydney central business district opposite the Queen Victoria Building and alongside St Andrew's Cathedral. Sited above the Town Hall station and between the city shopping and entertainment precincts, the steps of the Town Hall are a popular meeting place. It was designed by John H. Wilson, Edward Bell, Albert Bond.

G.4 VisualNews

Query: Former California officer Jay Cicinelli puts his head in his hands immediately after hearing the not guilty verdict in murder trial of a homeless man.

825 CLIP Top-5 Results

822

823 824

847

855

856

857

858

859

860 861

862

826 Rank No. 1, Cosine Similarity = 0.4364, Modality = text

In this courtroom sketch, a solemn scene unfolds as the individual is depicted during the sentencing phase of a high-profile trial. The person was sentenced to death, marking a significant moment in the judicial process. The courtroom, filled with tension and gravity, reflects the serious nature of the proceedings. The sketch captures the atmosphere and the weight of the decision rendered by the court.

832

833 Rank No.2, Cosine Similarity = 0.4186, Modality = text

The image shows a former general, who has been sentenced to life in prison for his role in the murder of a Catholic bishop during Argentina's 1976–83 military dictatorship. The trial revealed documents, including letters from the Vatican archives provided by Pope Francis, which showed the bishop's denunciation of the regime's abuses. The general was found guilty of ordering the murder of Bishop Enrique Angelelli in 1976, marking a significant conviction of a junta-era official for the killing of a high-ranking cleric.

840 ______

Rank No.3, Cosine Similarity = 0.3994, Modality = text

On October 3, 2011, in a courtroom filled with emotional tension, Amanda Knox's father is embraced by his wife following the announcement that Amanda had won her appeal against her murder conviction. The atmosphere is charged with relief and joy as supporters and family members react to the verdict. The image captures a poignant moment of familial support and celebration amidst the wider context of a highly publicized and dramatic legal battle.

848 Rank No.4, Cosine Similarity = 0.3718, Modality = text

Sudheendra Kulkarni was attacked with black ink, leaving his face and head covered. This incident occurred in public, attracting media attention and police presence, as seen in the image. Kulkarni was subsequently taken to a hospital to have the ink removed. The event highlighted tensions and provoked widespread reactions, underscoring the volatile nature of public discourse.

853

854 Rank No.5, Cosine Similarity = 0.3698, Modality = text

The Rev Sidney Davis leads mourners in a community prayer service at Second Presbyterian Church in Charleston, following the tragic shooting that claimed the lives of nine black worshipers. This gathering reflects the communal grief and solidarity in the face of violence, as mourners join hands in prayer. The event underscores ongoing discussions about race and gun control, issues highlighted during President Obama's presidency. The somber atmosphere is a reminder of the challenges and unresolved issues surrounding racial tensions and gun violence in America.

GR-CLIP Top-5 Results

Rank No.1, Cosine Similarity = 0.4265, Modality = image (Ground truth)



866 Rank No.2, Cosine Similarity = 0.3605, Modality = text

In this courtroom sketch, a solemn scene unfolds as the individual is depicted during the sentencing phase of a high-profile trial. The person was sentenced to death, marking a significant moment in the judicial process. The courtroom, filled with tension and gravity, reflects the serious nature of the proceedings. The sketch captures the atmosphere and the weight of the decision rendered by the court.

Rank No.3, Cosine Similarity = 0.3365, Modality = text

The image shows a former general, who has been sentenced to life in prison for his role in the murder of a Catholic bishop during Argentina's 1976–83 military dictatorship. The trial revealed documents, including letters from the Vatican archives provided by Pope Francis, which showed the bishop's denunciation of the regime's abuses. The general was found guilty of ordering the murder of Bishop Enrique Angelelli in 1976, marking a significant conviction of a junta-era official for the killing of a high-ranking cleric.

880

Rank No.4, Cosine Similarity = 0.3224, Modality = multimodal



MPs are raising concerns about the lack of access to inpatient mental health services for young people, highlighting cases like Nikki Mattocks, who faced significant delays and inadequate support. Despite her struggles with severe mental health issues, she experienced a fragmented care system, resulting in repeated emergency visits and admissions to distant psychiatric units. This lack of continuity and proximity to family exacerbated her condition. The parliamentary report underscores the urgent need for early intervention and better resource allocation to prevent further harm to vulnerable youths.

Rank No.5, Cosine Similarity = 0.2956, Modality = text

On October 3, 2011, in a courtroom filled with emotional tension, Amanda Knox's father is embraced by his wife following the announcement that Amanda had won her appeal against her murder conviction. The atmosphere is charged with relief and joy as supporters and family members react to the verdict. The image captures a poignant moment of familial support and celebration amidst the wider context of a highly publicized and dramatic legal battle.